N64109
Paper No.
60—WA-77

Shock Losses in Transonic Compressor Blade Rows

GENEVIEVE R. MILLER
GEORGE W. LEWIS, JR.
MELVIN J. HARTMANN
Lewis Research Center, National Aeronautics and Space Administration, Cleveland, Ohio

Introduction

Subsonic compressors were, for many years, limited to relative flow velocities equal to a Mach number of 0.75 or below. This limitation was a result of increasing losses, which occurred above this relative Mach number and, for the low energy additions utilized, caused a sizable loss in compressor efficiency. However, by the use of blade shapes less susceptible to shock losses, good compressor performance was obtained with a transonic compressor (ref. [1])[1] in which the tip relative flow velocity was slightly supersonic. The data from this early transonic compressor seemed to be a simple extension of that obtained from subsonic compressors. The loss data obtained from this transonic compressor rotor could be correlated with subsonic compressor losses by use of the loading parameter D factor. The D factor is described in reference [2] and defined in the symbol list in the Appendix. Because of this correlation, it was felt that the shock losses in this transonic compressor rotor were negligible. However, as more data became available over a wider range of loadings, Mach numbers, and solidity it was obvious that the D factor was not sufficient to establish design conditions of transonic compressors. A study was made of the blade element loss taken from 14 transonic compressor rotors in reference [3]. Fig. 1 is reproduced from reference [3] in which the tip element loss has been plotted against the D factor for minimum loss operation. Superimposed on this plot is the usual loss band as shown in the D factor report (ref. [2]). It is apparent that the bulk of the transonic data falls well above the loss coefficient band established by the D factor. Since all these data have supersonic relative inlet Mach numbers, it seemed reasonable to suspect that the higher loss is related to the shocks encountered in the blade row. An inspection of these data indicated that the increase in flow over that predicted by the D factor band was not a simple function of the relative inlet Mach number. That is, some of the higher relative Mach number points fall close to the band, whereas relatively low Mach number points fell above the band. It was also observed that a reduction of solidity caused a rapid increase in loss. Therefore, if these losses are to be related to the shock in the rotor passage, the effect of solidity and blade shape, as well as relative inlet Mach number, must be considered in the correlation.

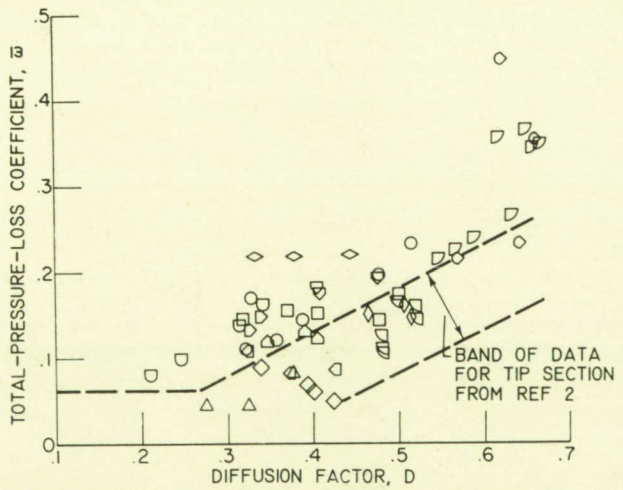

Fig. 1 Variation of the tip element total-pressure-loss coefficient with diffusion factor of rotors from reference [3]

[1] Numbers in brackets designate References at end of paper.

Contributed by the Gas Turbine Power Division for presentation at the Winter Annual Meeting, New York, N. Y., November 27–December 2, 1960, of The American Society of Mechanical Engineers. Manuscript received at ASME Headquarters, July 26, 1960. Paper No. 60—WA-77.

The object of this study is to obtain a physical understanding of the nature of the shock losses, to correlate these losses, and to determine methods of predicting the losses in transonic blade rows. The approach will be to review several studies of shock losses in transonic compressors and to compare the results of these studies with an analytical solution of the flow field. A simple flow model for estimating blade element shock losses was utilized in reference [3]. In addition, two experiments were conducted to obtain an understanding of the shock configurations in transonic blade rows. A hot-wire anemometer was utilized to determine the blade-to-blade loss distribution in a rotor with shock losses in reference [4]. High-frequency-response barium titanate crystals were used to indicate shock location in the blade passage in reference [5]. Finally, a method utilizing estimated shock losses for design of transonic blade rows was suggested by the analysis.

A Simple Flow Model for Estimating Shock Losses

To estimate the magnitude of the shock loss, a shock pattern or configuration as shown in Fig. 2 was assumed (from ref. [3]). In this case, the shock was assumed to stand near the entrance of the blade passage, striking the suction surface at the point B, extending in front of the blade at point A, and then bending back similar to a bow wave. It was then assumed that the loss across this shock could be approximated by the normal shock loss taken for the average of the Mach numbers at points A and B. The Mach number at point A was assumed to be equal to the inlet relative Mach number. The Mach number at B would be somewhat higher because of the turning along the blade suction surface. This Mach number can be calculated from the upstream relative Mach number and flow direction and the angle of turning along the suction surface to point B (expansion waves along blade surface). To obtain the turning to this point, it is necessary to have a consistent and reasonable method of locating B. This location was chosen as the intersection of the suction surface and a line drawn normal to the mean passage camber line and through the leading edge of the next blade. Note that the location of B is affected by blade spacing. If the blades are moved farther apart (lower solidity), point B falls farther back from the blade leading edge. Thus, the loss calculated from the average Mach number is a function of relative inlet Mach number and blade row solidity, which were two parameters observed to affect

Discussion on this paper will be accepted at ASME Headquarters until January 10, 1961

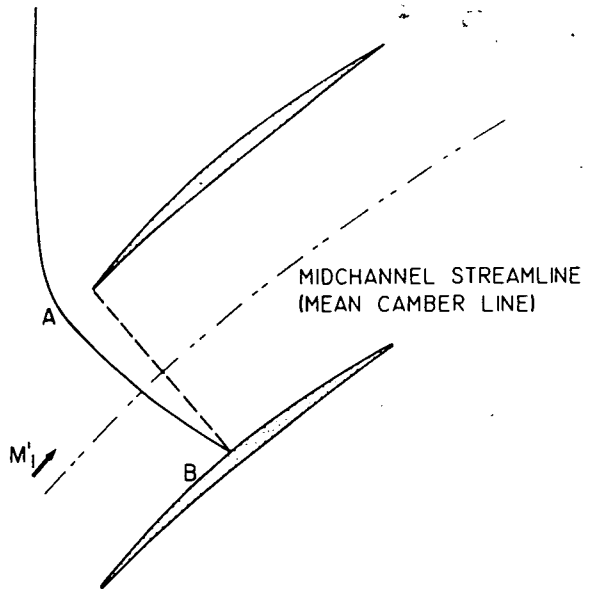

Fig. 2 Passage shock-wave configuration for estimating shock-loss levels

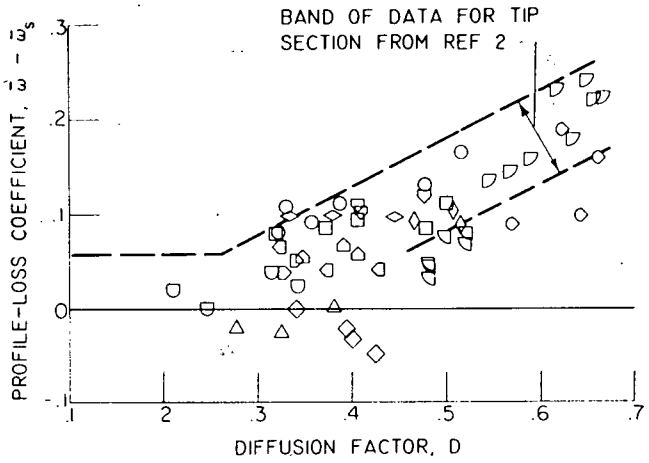

Fig. 3 Variation of tip element profile losses with diffusion factor of rotors from reference [3]

the distribution of the measured loss data, as discussed from Fig. 1.

The method for estimating shock loss values described above was applied to the data from the 14 transonic compressor rotors of reference [3]. Even with the assumptions involved in the averaging method, some interesting results were obtained pertaining to the magnitude of shock losses, as shown in Fig. 3. The shock losses calculated by the method just described have been subtracted from the over-all measured losses and are plotted here as a difference or profile loss coefficient against diffusion factor. When this was done, the profile loss fell within or below the usual D factor band (Fig. 3). From this it was concluded that the shock losses were the major factor causing the scatter of loss data above the D factor loss band. The suction-surface Mach number at point B (indicated in the previous figure) was surprisingly high, resulting in Mach numbers in the order of 1.8 for many of the high loss points. At such Mach number levels, shock-boundary-layer interactions undoubtedly result in separation from the blade suction surface. Under such circumstances, it is really surprising that the profile loss, or difference between the total measured loss and estimated shock loss, falls in the D factor band, which was determined as the total loss coefficient at subsonic Mach numbers. However, the consistent nature of the data falling into the D factor band merits some further consideration.

The reference report subsequently showed that shock losses as calculated constituted 0.35 to 0.55 of the total loss. All the data shown in the figures were for tip element performance; however, at other supersonic blade elements the same percentages of loss (0.35 to 0.55) were attributed to the shock. Thus, it becomes apparent that shock loss can be of such a magnitude that it must be considered in the design of transonic rotors.

Blade-to-Blade Loss Distribution

In the previous discussion it was indicated that blade row losses can be divided into two loss coefficients. Namely, those losses associated with the blade profile $\bar{\omega}_p$ and those associated with the passage shock $\bar{\omega}_s$. The profile losses would result in a total-pressure distribution behind a blade row as shown in Fig. 4. This type of total-pressure distribution was obtained by the use of a hot-wire anemometer in reference [6]. In this case, the losses are concentrated in the blade wake regions and the free-stream region is relatively loss free. In fact, it has been shown in reference [6] that, if the free-stream loss is taken as zero and the loss distribution is integrated, the wake loss is equal to that measured by the usual instrumentation downstream of the blade row. If, however, there is a shock across the passage, the free-stream loss is no longer equal to zero. This is shown in Fig. 5. At the top of the figure, a blade row operating at supersonic relative Mach numbers is indicated with a series of expansion waves followed by a passage shock. Under such conditions, the total pressure in the free stream must vary from a rather low value on the suction surface to a rather high total pressure near the nose of the next blade because of the variation of passage shock loss, that is, the loss of the passage shock would vary according to the Mach number ahead of the shock. Now if this total-pressure distribution in the free stream is superimposed on that of the subsonic blade row, in which only profile losses appeared, a total-pressure distribution such as that shown at the bottom of Fig. 5 would be obtained. The blade wake is represented by the region of low total pressure. The total pressure gradually increases from the suction surface toward the pressure surface where another wake region is encountered. Thus, the total-pressure distribution shown at the bottom of the figure is that which would be expected when shock losses are encountered.

The data of Fig. 6 are based on the results of hot-wire anemom-

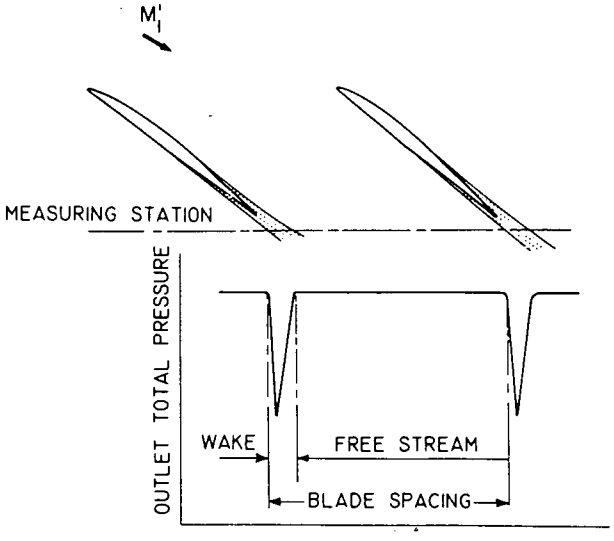

Fig. 4 Variation of total pressure downstream of a blade row

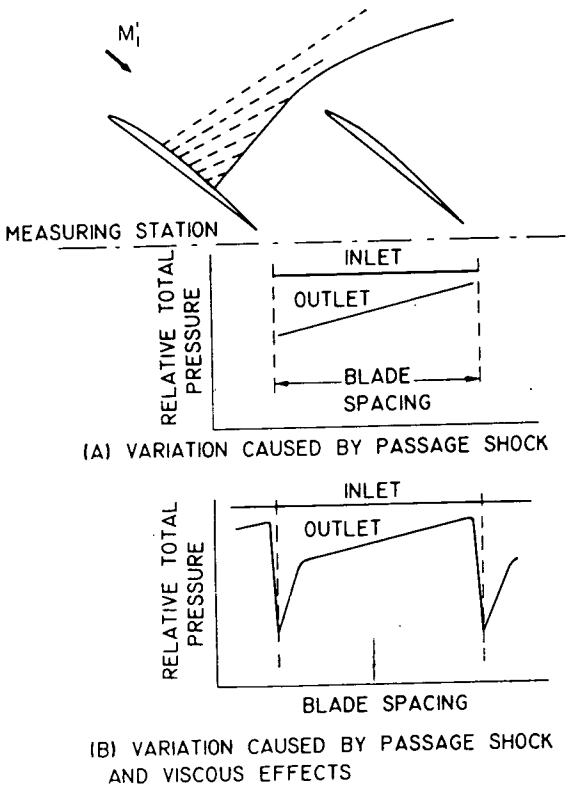

Fig. 5 Circumferential variation of relative total pressure at outlet of blade element operating with supersonic inlet relative Mach numbers

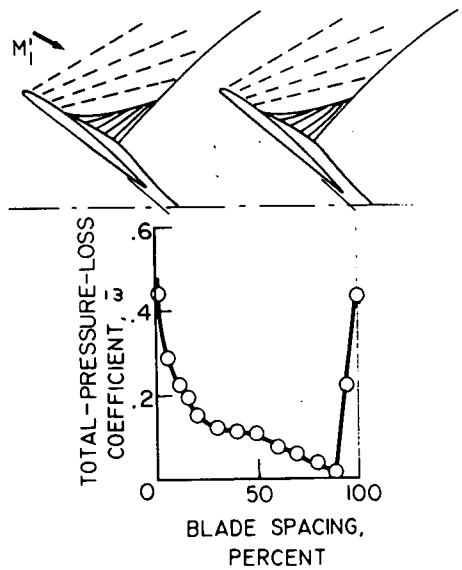

Fig. 6 Blade-to-blade loss distribution in flow with passage shock as indicated by hot-wire anemometer

eter data taken behind a blade row operating at supersonic relative Mach numbers (from ref. [4]). In this case, however, the hot-wire measurement is converted to a total-pressure loss coefficient plotted against per cent of blade spacing. This particular plot is for a transonic rotor with a tip solidity of about 0.83 operating at a tip speed of about 1100 feet per second and near the point of maximum efficiency. The region between the blades (which is normally the free-stream flow) shows a varying loss coefficient, being relatively high near the blade suction surface (0 per cent blade spacing) and decreasing toward the pressure surface (90 per cent blade spacing). The high losses at the two sides of the passage represent the profile loss regions. A sketch of the shock configuration probably associated with this loss distribution is shown at the top of Fig. 6. Near the nose of the next blade (pressure surface) the Mach number of the shock is relatively low, approximately inlet relative Mach number, and the shock loss associated with this region is small. As the shock approaches the suction surface of the blade, the Mach number ahead of the shock continues to increase and thus the loss coefficient shows a gradual rise. These hot-wire data show a change in slope near the middle of the passage. This may be explained by the shock configuration above, which illustrates a considerable shock-boundary-layer interaction. Under such circumstances, the static-pressure rise across the shock, being relatively high, is felt back through the boundary layer along the suction surface of the blade, causing the boundary-layer thickness to increase upstream of the shock. This requires the flow to bend away from the wall through a series of compression waves which coalesce to form the shock in the free stream. The losses associated with this gradual compression are somewhat smaller than normal shock losses at the theoretical Mach number without boundary-layer compression waves. In general, the loss distribution obtained from the hot-wire trace confirms a Mach number variation ahead of the shock similar to that used in the simple flow model of reference [3].

Shock Configurations in Rotor Tip Regions

Experimental data which substantiate the shock configuration used in the simple flow model were obtained from high-frequency, static-pressure transducers and presented in reference [5]. An installation of these barium titanate crystal pickups is sketched in Fig. 7. Four crystal pickups were located along the wall of the rotor housing. The dashed lines indicate the blade-to-blade path surveyed by each crystal, the first crystal being near the leading edge and the others located at various axial positions as shown. In Fig. 8 some oscilloscope traces from the static-pres-

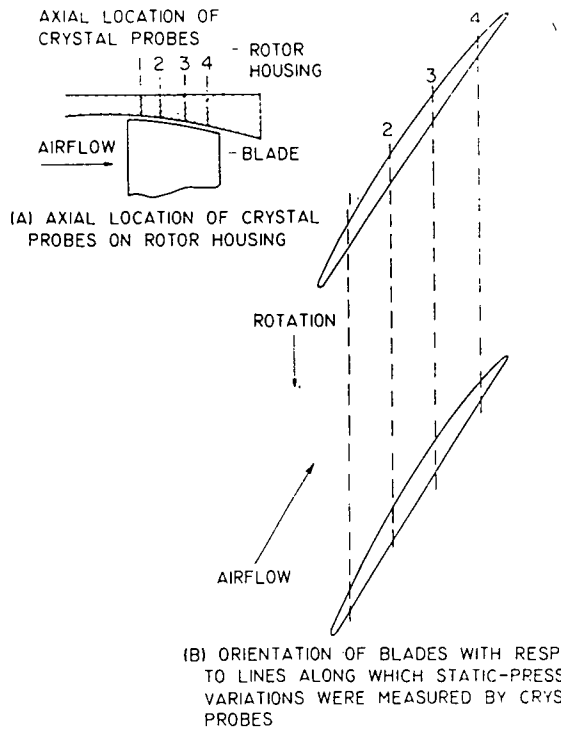

Fig. 7 Location of barium titanate crystal probes for indicating static pressure variations at blade tip

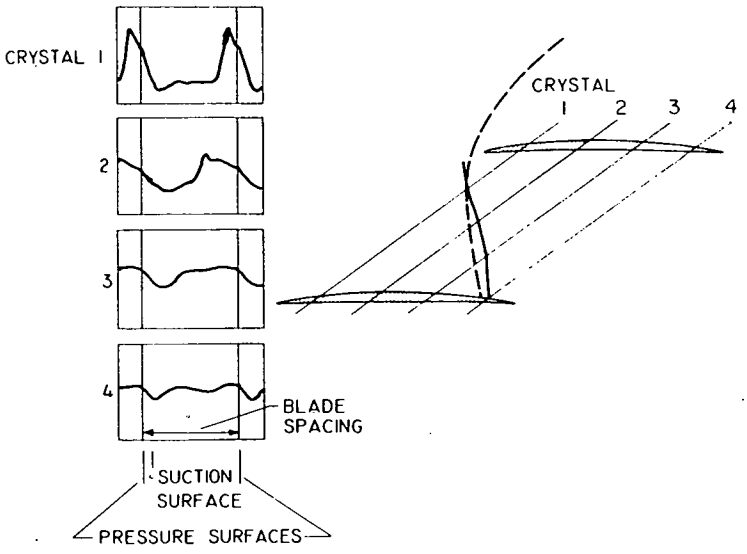

Fig. 8 Oscilloscope traces taken at the four crystal-probe stations and used to locate shock pattern in transonic rotor operating at design speed near maximum efficiency

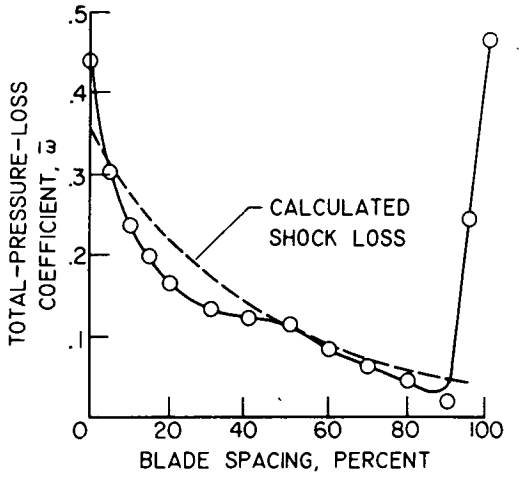

Fig. 10 Comparison of blade-to-blade loss distribution measured with a hot-wire anemometer and calculated by the detailed shock model

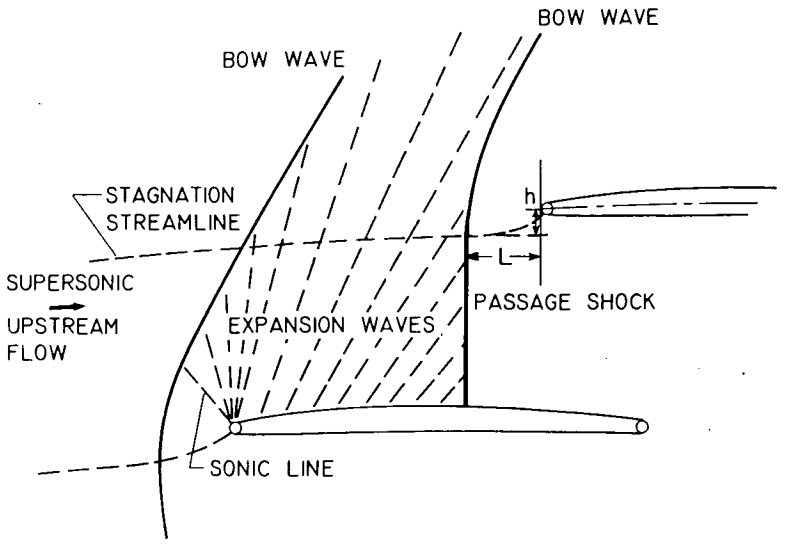

Fig. 9 Flow at inlet of cascade f airfoils operated with supersonic relative inlet Mach number

sure crystal pickup are shown. The static pressure decreases rapidly as the blade passes the crystal, followed by a gradual build up in pressure as the pressure surface approaches. The sudden rise in pressure between the blades indicates the presence of a shock. The location of this sudden static-pressure rise or shock relative to the blades was used to locate the passage shock. The shock shape and location as determined by these crystal pickups is shown by the solid line in Fig. 8 for an operating point near maximum efficiency of the particular rotor used in this investigation. Also shown on Fig. 8 for comparison is a dotted line indicating the approximate shock shape and location assumed in the simple flow model used to estimate shock losses. It can be seen that the shock location obtained from the crystal data is very close to that assumed in the simple flow model.

A More Detailed Model for Calculating Shock Losses

It has been shown by two experimental techniques that the shock configuration assumed for the simple flow model is similar to that which exists at the design point for a transonic compressor rotor. Also, it was indicated that some rough approximations to the loss obtained over this flow model gave reasonable experimental correlations. Still to be obtained, however, are a more comprehensive evaluation of the flow conditions and refinement of the loss estimates associated with this shock configuration. The more complete evaluation of flow conditions and shock losses will be described from Fig. 9, a two-dimensional sketch of the flow field and a similar shock model, which can be utilized for a more detailed calculation of the shock losses (as given in ref. [5]). The dashed lines represent Mach lines in the expansion region obtained over the suction surface of the blade as determined by the upstream flow Mach number, flow direction, and the turning on the suction surface of the blade. Along each of these Mach lines, the flow is assumed to be parallel to the blade suction surface at the origin of the line. The flow Mach number and direction are thus determined everywhere in the expansion field. The flow quantity for this blade passage is known from the upstream flow conditions. Since the flow conditions along each of the expansion lines are also known, continuity will establish the stagnation streamline through the supersonic flow region. This solution can be extended back to the passage shock. A

theory of bow waves on cowl lips for supersonic inlets was used to establish the intersection of the shock line with the stagnation streamline (ref. [5 and 7]). It requires a knowledge of the upstream Mach number and the streamline deflection behind the shock, shown as h in this figure, and results in an evaluation of the length L or the distance the bow wave stands ahead of the blade. This theory was based on bow waves of isolated bodies for which the upstream Mach number was constant. For the case of a blade row, however, the Mach number is varying slightly along the face of the shock. For this analysis the Mach number was assumed to be that calculated on the stagnation streamline at the face of the shock.

A previous investigation (ref. [5]) calculated the losses associated with the portion of the bow wave extending beyond the stagnation streamline and indicated that for small incidence angles these losses were relatively small compared with the passage shock losses. Therefore, this discussion will deal with the passage shock losses only (between the blade and stagnation streamline). Now that the origin of the shock is established, it is necessary to assume a direction taken by the passage shock. For the purposes of this analysis, it was assumed that the shock direction was the same as that of a line drawn through the nose of the leading edge of the blade and extending across the blade passage normal to the mean passage camber line. Thus, the necessary assumptions have been made to define the shock shape and location. The Mach number and flow direction are available all along the face of the assumed passage shock. Then the loss variations along the shock can be established and a mass averaged shock loss can be obtained. It should be noted that this shock shape and location is slightly different from that used in the initial calculations. We now have an analytical two-dimensional method for predicting the flow field and shock losses in a transonic blade row. Some results of calculations made by this method will be compared with experimental data obtained at the point of minimum loss operation.

The loss distribution from blade to blade can be computed and is shown on Fig. 10 along with measured loss distribution. The total-pressure loss coefficient is plotted against blade spacing. The measured data are the same hot-wire data as previously shown. It can be seen that, in the midpassage region, the shape of the calculated loss distribution is very close to that obtained from the hot-wire anemometer. The analytical method just described does not account for boundary-layer shock interactions and thus does not show the dip near the suction surface as indicated on the hot-wire anemometer trace. However, this comparison indicates that the shock shape and strength assumed must be reasonably close to that existing at the design conditions.

Comparison of Experimental and Analytical Shock Losses

Now that some confidence has been gained from experimental evidence supporting both the simple flow model and the more detailed flow model shock loss estimates, the magnitude of losses obtained from these methods must be compared. In the table of Fig. 11, such a comparison can be made for the minimum loss points of tip elements of a representative sample of transonic compressor rotors. The operating conditions of these blade elements are indicated here as element relative Mach number and D factor. It can be noted that, for this sample of data, the D factor ranged from about 0.34 to 0.55 and the relative Mach number ranged from 1.07 to about 1.28. The estimated shock losses obtained by the simple flow model (column 5, $\bar{\omega}_s$) and the shock losses obtained by the more detailed method (column 6, $\bar{\bar{\omega}}_s$) are compared on Fig. 11. The loss coefficients agree surprisingly well for these data. The magnitude of shock loss estimated ranges from about 0.04 to 0.14 for the simple flow model and thus a representative range of shock losses has been obtained

1	2	3	4	5	6	7	8	9
REFERENCE	RADIAL DISTANCE FROM TIP, PERCENT	INLET RELATIVE MACH NUMBER	DIFFUSION FACTOR, D	TOTAL-PRESSURE LOSS				
				CALCULATED				MEASURED OVERALL LOSS, $\bar{\omega}$
				SIMPLE SHOCK MODEL, $\bar{\omega}_s$	DETAILED SHOCK MODEL, $\bar{\bar{\omega}}_s$	PROFILE LOSS, $\bar{\omega}_p$	ESTIMATED TOTAL LOSS, $\bar{\omega}_s + \bar{\omega}_p$	
8	13	1.070	0.514	0.057	0.053	0.119	0.176	0.145
8	13	1.081	.476	.074	.066	.099	.173	.193
9	11	1.128	.545	.079	.076	.134	.213	.215
10	10	1.074	.373	.041	.047	.047	.088	.082
10	10	1.066	.407	.063	.052	.064	.127	.121
11	11	1.282	.343	.139	.156	.031	.170	.163

($\bar{\omega}_p$), LOSS FROM CURVE FAIRED THROUGH DATA OF FIG. 3

Fig. 11 Table of calculated and measured total-pressure losses for transonic compressor rotors

in these sample data. It may be assumed that for the range of variables shown above it is not necessary to use the more detailed flow calculation to obtain the design-point shock-loss coefficient.

Considering the simple flow model, it was suggested that for design-point operation a reasonable approximation to the total loss would be obtained if a shock loss was added to the profile loss. The profile loss for these data was taken from a mean line drawn through the data obtained from the 14 transonic compressor rotors previously described in Fig. 3 (and ref. [3]). This is tabulated in the column designated "Profile loss" (column 7). In the next column (8), the profile loss has been added to the shock loss as determined by the simple flow model. The last column is measured loss coefficient. It can be noted that in general the predicted loss coefficient is close to the measured loss coefficient. This method of loss superposition seems to be a reasonable method for predicting the losses in transonic blade rows.

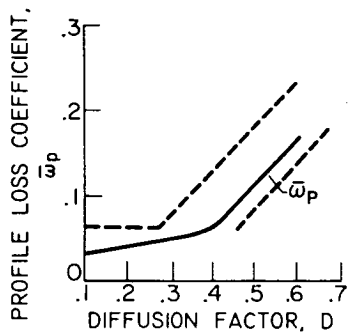

Fig. 12 Profile loss curve faired through data points from Fig. 3

As a matter of interest, the profile loss used in preparing this table is shown in Fig. 12. This represents the mean profile loss for the tip element of the 14 transonic compressor rotors. This mean line is about one-third of the distance between the band width given for the D factor loss correlation. The comparison in the table of Fig. 11 of the estimated loss (column 8) and the measured loss (column 9), is influenced greatly by the fairing of this curve through the profile loss data.

Shock Losses at Various Rotor Radii

In some transonic rotor designs, blade elements at radii below the tip element are operating at supersonic relative Mach numbers and shock losses should be considered. The magnitude of this problem can be indicated in Fig. 13. The relative inlet Mach numbers for three transonic compressors have been plotted

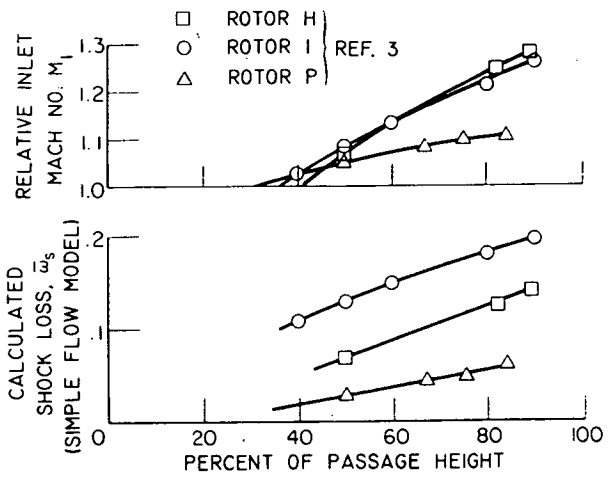

Fig. 13 Radial distribution of inlet relative Mach number and shock loss for three transonic compressor rotors

against per cent of discharge passage height. (These data are from rotors I, H, and P of ref. [3].) The lower part of Fig. 13 shows estimated shock loss coefficients (simple flow model). It can be observed that the calculated shock loss can be large even though the inlet relative Mach number is sonic at reduced radii (0.50 or 0.40 radius ratio). Apparently, significant shock losses can occur even at relative inlet Mach numbers of the order of 1.

The effect of shock loss along the radius can be seen somewhat better in Fig. 14 where the various loss components are plotted against radius ratio for rotor H of Fig. 13. The dashed line is a replot (from Fig. 13) of the shock losses calculated by the simple flow model. The dotted line is the distribution of profile losses determined from the profile loss curve shown in Fig. 12.

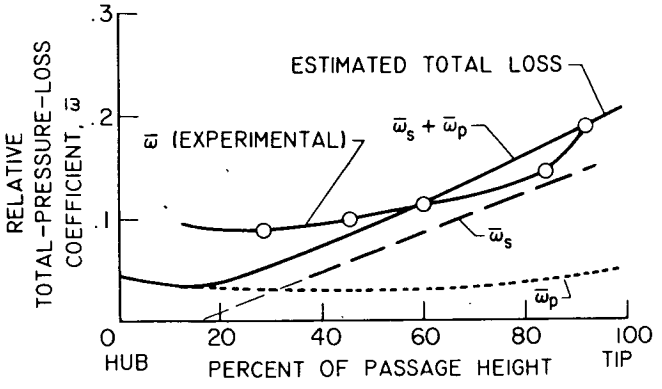

Fig. 14 Radial distribution of shock and profile losses of transonic compressor rotor H of reference [3]

The profile loss curve is faired upward in the rotor hub region to the upper edge of the D factor loss band to account for the hub effects not previously considered. These two loss components have been added together to obtain a total loss distribution, shown as the solid line in Fig. 14. This line, which would be considered as the design loss distribution, compared reasonably well to the measured loss distribution shown on this figure.

Variation of Calculated Shock Losses With Incidence

Since the methods of predicting shock losses at the design point seem adequate, it is desirable to consider the effect of shock losses at off-design conditions. The detailed flow model described above lends itself to analysis over a range of operating conditions. This method requires only a knowledge of the upstream Mach

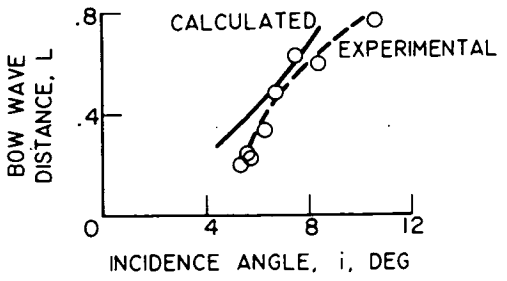

Fig. 15 Off-design bow waves distance versus incidence angle for transonic compressor rotor H of reference [3]

number, the flow angle, and the blade geometry in order to determine the shock location and to estimate the magnitude of shock loss.

The dimensionless distance L that the bow wave stands ahead of the blade leading edge for the rotor of reference [5] was calculated over a range of incidence angles and is compared with the measured distance in Fig. 15. The measured distance was obtained from crystal probes previously described and indicates that the theory reasonably well predicts the shock location over a range of incidence angles. Some other rotors for which such data were available have indicated measured shock distances somewhat greater than the predicted distance; however, the difference between the measured and calculated locations was small. This agreement between predicted and measured conditions was encouraging and indicated that the analytical method has some validity over a range of incidence angles. The method was then used to estimate the variation of shock losses at the tip of one transonic rotor at these off-design operating conditions.

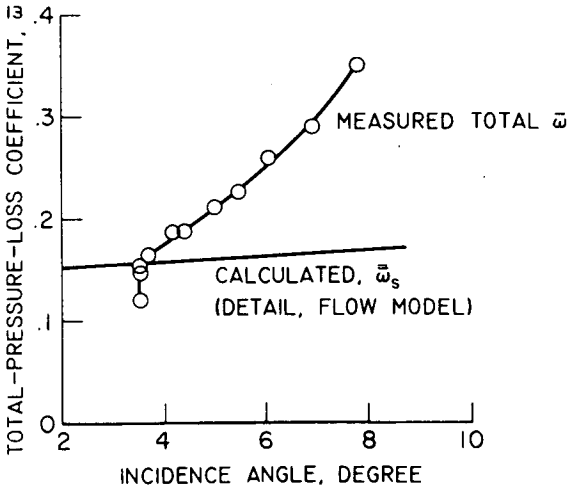

Fig. 16 Typical variation of total-pressure-loss coefficient with incidence angle for transonic compressor rotor H of reference [3]

The results are shown in Fig. 16. The estimated shock loss does not vary appreciably over the range of incidence angles. This is the result of the fact that, as the incidence angle increases, the shock moves forward so that the Mach number at the shock remains essentially constant. Also shown on Fig. 16 is the measured element loss for the blade row tip element. The measured total blade element loss increases very rapidly with incidence angle. Thus, the trend of rapidly increasing loss with incidence angle was apparently not primarily the result of increasing shock losses. If the calculated shock loss at the off-design incidence is reasonably correct, the large loss change with incidence angle must be due to a large change in profile loss. Into these profile losses have been lumped the viscous loss and the large unknown,

shock boundary layer interaction effects. It has been shown in subsonic compressor rotors and cascade tests that the profile losses do increase in this manner with incidence (for example, fig. 10, ch. 7, ref. [12]). It should also be pointed out that the more complete methods of predicting losses over a range of incidence angles (D factor applies only at design incidence angle) as given in reference [13] would probably indicate a loss increase similar to that measured.

Remarks

The simple flow model is adequate for predicting the magnitude of shock losses in transonic compressor blade rows at or near design point operation. The more detailed flow model did result in a better understanding of the flow conditions in a transonic blade row, and to some extent may be useful to predict shock losses over a range of blade incidence angle. However, since the entire shock loss analysis has been based on the two-dimensional blade element approach, further refinement of such simplified methods of predicting the shock losses probably would not improve the understanding of the flow conditions or the prediction of transonic compressor performance.

It should be kept in mind that the methods used were developed to understand and improve the correlation data from 14 transonic compressor rotors. All examples shown were data used in the over-all correlation. Although these methods seem equally applicable to predict the performance of similar machines, it is not known to what extent these correlations apply outside the range of variables (Mach number, solidity, etc.) covered by these 14 transonic compressor rotors.

Summary of Results

The rather extensive study of the shock losses in transonic compressors can be summarized by the following remarks:

1 A simple flow model can be used to estimate shock losses at the design point for transonic compressor blade rows and results in reasonable correlation of loss data. It is indicated that shock losses can constitute a sizable portion of the total losses in a transonic compressor rotor. This includes all blade elements at which sonic or higher relative velocities are obtained.

2 Shock losses can be shown to exist across the blade passage (free-stream loss) and by the method of superposition with the blade profile losses result in an estimated design total loss coefficient.

3 The shock configuration was experimentally determined by the rapid pressure rise between the blades as measured by the use of barium titanate crystals. At the minimum loss operating conditions the shock is very similar to that assumed in the simple flow model.

4 Shock losses obtained from a more detailed flow model were compared with the losses obtained by the simple flow model. Measured loss distribution from blade to blade closely approaches the analytical shock loss distribution. The measured distribution shows the effect of a shock boundary layer interaction.

5 The analytical method (from the detailed flow model) of determining the shock location ahead of the blade seems to apply reasonably well over a range of incidence angles. The analytical shock losses do not vary a great deal with blade element incidence angles.

APPENDIX

Symbols

D = diffusion factor, $D = 1 - V_2'/V_1' + V\theta/2V_1'\sigma$ (ref. [2])
i = incidence angle, angle between relative inlet-air direction and tangent to blade mean camber line at leading edge, deg
h = streamline deflection behind shock
L = distance of bow wave ahead of blade leading edge
M_1' = relative inlet Mach number
P = total pressure
p = static pressure
V = air velocity, ft/sec
σ = blade solidity, ratio of chord to spacing
$\bar{\omega}$ = relative total pressure loss coefficient, $(P_{2,i} - P_2)/(P_1 - p_1)$
$\bar{\omega}_s$ = calculated shock loss coefficient (total pressure) (simple flow model)
$\bar{\bar{\omega}}_s$ = calculated shock loss coefficient (total pressure) (detailed flow model)
$\bar{\omega}_p$ = profile loss coefficient, $\bar{\omega}_p = \bar{\omega} - \bar{\omega}_s$

Subscripts

1 = rotor inlet
2 = rotor outlet
i = ideal
θ = tangential direction

Superscripts

$'$ = relative to rotor
$-$ = mass-averaged value

References

1 Seymour Lieblein, George W. Lewis, Jr., and Donald M. Sandercock, "Experimental Investigation of an Axial-Flow Compressor Inlet Stage Operating at Transonic Relative Inlet Mach Numbers. I—Over-All Performance of Stage With Transonic Rotor and Subsonic Stators up to Rotor Relative Inlet Mach Number of 1.1," NACA RM E52A24, 1952.

2 Seymour Lieblein, Francis C. Schwenk, and Robert L. Broderick, "Diffusion Factor for Estimating Losses and Limiting Blade Loadings in Axial-Flow-Compressor Blade Elements," NACA RM E53D01, 1953.

3 Francis C. Schwenk, George W. Lewis, and Melvin J. Hartmann, "A Preliminary Analysis of the Magnitude of Shock Losses in Transonic Compressors," NACA RM E57A30, 1957.

4 George W. Lewis, Edward R. Tysl, and Theodore E. Fessler, "Analysis of Transonic Rotor-Blade Passage Loss With Hot-Wire Anemometers," NACA RM E58C04, 1958.

5 Genevieve R. Miller and Melvin J. Hartmann, "Experimental Shock Configurations and Shock Losses in a Transonic-Compressor Rotor at Design Speed," NACA RM E58A14b, 1958.

6 Theodore E. Fessler and Melvin J. Hartmann, "Preliminary Survey of Compressor Rotor-Blade Wakes and Other Flow Phenomena With a Hot-Wire Anemometer," NACA RM E56A13, 1956.

7 John F. Klapproth, "Approximate Relative-Total-Pressure Losses of an Infinite Cascade of Supersonic Blades With Finite Leading-Edge Thickness," NACA RM E9L21, 1950.

8 Francis C. Schwenk and George W. Lewis, Jr., "Experimental Investigation of a Transonic Axial-Flow-Compressor Rotor With Double-Circular-Arc Airfoil Blade Sections. III—Comparison of Blade-Element Performance With Three Levels of Solidity," NACA RM E55F01, 1955.

9 Francis C. Schwenk, George W. Lewis, Jr., and Seymour Lieblein, "Experimental Investigation of an Axial-Flow-Compressor Inlet Stage Operating at Transonic Relative Inlet Mach Numbers. V—Rotor Blade-Element Performance at a Reduced Blade Angle," NACA RM E56J17, 1957.

10 Edward R. Tysl and Francis C. Schwenk, "Experimental Investigation of a Transonic Compressor Rotor With a 1.5-Inch Chord Length and an Aspect Ratio of 3.0. III—Blade-Element and Over-All Performance at Three Solidity Levels," NACA RM E56D06, 1956.

11 John W. R. Creagh, "Performance Characteristics of an Axial-Flow Transonic Compressor Operating up to Tip Relative Inlet Mach Number of 1.34," NACA RM E56D27, 1956.

12 Members of Compressor and Turbine Research Division, "Aerodynamic Design of Axial-Flow Compressors," Vol. II, NACA RM E56B03a, 1956.

13 Seymour Lieblein, "Loss and Stall Analysis of Compressor Cascades," *Journal of Basic Engineering*, Series D, TRANS. ASME, vol. 81, 1959, pp. 387–397.

Printed in U. S. A.